Localization of CdSe/ZnS Quantum Dots in the lysosomal acidic compartment of cultured neurons and its impact on viability: potential role of ion release

Localization of CdSe/ZnS Quantum Dots in the lysosomal acidic compartment of cultured neurons and its impact on viability: potential role of ion release.

Ingrid Corazzari[a, c, d, 1], Alessandra Gilardino[b, c, 1], Simona Dalmazzo[b], Bice Fubini[a, c, d, *], and Davide Lovisolo[b, c, *]

[a] Department of Inorganic, Physical and Molecular Chemistry, University of Torino, via Pietro Giuria 7, 10125 Torino, Italy.

[b] Department of Life Sciences and Systems Biology, University of Torino, via Accademia Albertina 13, 10123 Torino, Italy

[c] Interdepartmental Center for Nanostructured Interfaces and Surfaces, University of Torino, via Pietro Giuria 7, 10125 Torino, Italy

[d] "G. Scansetti" Interdepartmental Center "for Studies on Asbestos and other Toxic Particulates, University of Torino, via Pietro Giuria 7, 10125 Torino, Italy

* to whom correspondence should be addressed:
Davide Lovisolo
Dept. of Life Sciences and Systems Biology
University of Torino
Via Accademia Albertina 13
10123 Torino Italy
davide.lovisolo@unito.it
phone ++39 011 6704668
fax ++39 011 6704508

Bice Fubini
Dept. of Chemistry
University of Torino
Via P. Giuria 7
10125 Torino Italy
bice.fubini@unito.it
phone ++39 011 6707566
Fax ++39 011 6707855

[1]These two Authors contributed equally to this work

Abstract

CdSe Quantum Dots (QDs) are increasingly being employed in both industrial applications and biological imaging, thanks to their numerous advantages over conventional organic and proteic fluorescent markers. On the other hand a growing concern has emerged that toxic elements from the QDs core would render the nanoparticles harmful to cell cultures, living animals and humans. Neurotoxicity in particular, needs to be carefully evaluated since nanoparticles can access the nervous system by several pathways, including the olfactory epithelium. The pH of the environment to which the nanoparticles are exposed may play a crucial role in the stability of QDs coating. For this reason we investigated the release of metal ions from CdSe/ZnS QDs in artificial media reproducing the cytosolic and lysosomal cellular compartments characterized respectively by a neutral and an acidic pH. In the latter significant amounts of both Cd^{2+} and Zn^{2+} were released. We provide evidence that these QDs are internalized in the GT1-7 neuronal cell line and located in the lysosomal compartment. These findings can be related to a slight but significant reduction in cell survival and proliferation.

Key words: Quantum Dots, neurons, Cd release, lysosomal incorporation, neurotoxicity

1. Introduction

CdSe Quantum Dots (QDs) have been shown to be an innovative tool for biological labelling, due to their bright fluorescence, narrow emission, broad UV excitation, size-tunable emission (from the UV to the IR) and high photostability (Chan and Nie, 1998; Bruchez et al. 1998; Chan et al., 2002). Several groups have proposed the application of QDs to fluorescence imaging of single cells, subcellular structures and whole organs in *in vitro* and *in vivo* models (Ballou et al., 2004). These applications are predicted to grow thanks to their numerous advantages over alternative biological labelling moieties (e.g. fluorescent dyes and radioisotopes) (Yang et al., 2011; Akerman et al., 2002; Dubertret et al., 2002; Larson et al. 2003). As the popularity of QDs labelling soars, there is a growing concern that toxic elements of the QDs core (e.g. cadmium, selenium) would render the nanoparticles harmful to both cell cultures and live animals.

The available literature highlights that assessing QDs exposure routes and potential toxicity is not a simple matter because not all QDs are alike and toxicity depends upon multiple physicochemical as well as environmental factors (Hardman, 2006). Nowadays human exposure to QDs through the direct administration for therapy or diagnostic purposes has not yet been exploited. Human exposure so far is mostly undesired, i.e. environmental or occupational even if biomedical applications are foreseen. Thus the only route of exposure of toxicological interest is presently through dermal contact, ingestion and inhalation (Hardman, 2006).

The mechanism(s) potentially involved in cell death are not well understood. Cell toxicity is probably due to the presence of free Cd^{2+} ions from core degradation. However some adverse interactions of QDs with intracellular components leading to loss of cell function (Hardman, 2006; Kirchner et al., 2005; Derfus et al., 2004) may also play an important role. The involvement of reactive oxygen species (ROS) claimed by some authors in the mechanism of QDs toxicity (Derfus et al., 2004) is controversial, depending on particular conditions of photoirradiation and on QDs composition (Ipe et al., 2005). CdS Qds may generate both superoxide and hydroxyl radicals while CdSe Qds generate mainly hydroxyl radicals. Derfus et al. (2004) reported that CdSe particles suspended in aqueous solution release Cd^{2+} ions, with concentration directly related to citotoxicity. In the same study the authors evidenced that ion release is enhanced by oxidative and photolytic conditions (i.e. oxygen, UV irradiation) which may cause a dissolution of CdSe.

A direct way to avoid the citotoxic effects of QDs is thus to make them biologically inert by means of an efficient coating. The encapsulation of CdSe QDs with a ZnS shell or other stable capping materials has proved to be, at least partially, an efficient approach in reducing their toxicity (Derfus et al., 2004; Rzigalinski and Strobl, 2009).

Some studies on ZnO nanowires suggested that the toxicity of such nanoparticles is due to the release of Zn^{2+} ions which exert a toxic effect (Muller et al., 2010); similarly the Zn^{2+} released in solution from the shell may play a role in the QDs toxicity.

Some studies suggested that secondary coatings in addition to ZnS may better prevent Cd^{2+} leakage from the core (Derfus et al., 2004) than the simple ZnS one. However the stability of the capping materials may decrease under oxidative and photolytic conditions exposing the potentially toxic shell material and core metal components (Derfus et al., 2004). On the other hand, some Authors have proposed that toxicity is mainly dependent on the capping material (Derfus et al., 2004; Hoshino et al., 2007; Clift et al., 2010). Among the different coatings, PEG-capped QDs appear to be the less toxic (Zhang et al., 2006; Ryman-Rasmussen et al., 2007), even if there is not complete agreement on this issue. An early comprehensive review of QDs cytoxicity on non neuronal cells can be found in Lewinski et al., 2008.

A chemical parameter that may play a crucial role in the stability of QDs coating is the pH of the environment to which the nanoparticles are exposed. The available studies suggest that QDs are stable materials when used in their intended applications at near-neutral pH, but various types of QDs under acidic (pH 4) or alkaline (pH 10) conditions rapidly release cadmium and selenide ions following QD destabilization upon loss of the organic coating (Mahendra et al., 2008). The importance of monitoring the behaviour of QDs at different pH resides in the wide biodistribution of these nanoparticles in the whole body (*in vivo* tests) or in the different cellular subcompartments such as lysosomes, endosomes and cytosol.

In this light the aim of this work was to investigate the stability of the coatings of QDs in biosimulated fluids paradigmatic of what these nanoparticles may be in contact with when they reach tissues and cells. The neutral extracellular/cytosolic environment and the acidic environment of subcellular structures such as endosomes and lysosomes - the vesicles involved in the processes of endo- and phagocitosis - have been considered. The incorporation and subcellular localisation of these QDs in a neuronal cell model, the GT1-7 cell line, employed by our group in several studies (see *e.g.* Ariano et al., 2011), provided evidence for an albeit partial localisation in lysosomes, which is in agreement with the observed limited functional effects.

Since pharmacokinetic studies evidenced that carboxyl-QDs were detected in significantly higher amounts than amine- or PEG-QDs in heart, lung, liver, spleen, skeletal muscle, thoracic aorta, and brain (Praetner et al., 2010), we chose to study two commercial ZnS/CdSe QD samples coated with a polymer which has $–COO^-$ groups on its surface, Qdot® 525 ITK™ carboxyl and Qdot® 585 ITK™ carboxyl quantum dots from Invitrogen (Carlsbad, CA) hereafter named QDs 525 and QDs 585 respectively.

The choice of a neuronal model is of particular relevance, since high neurotoxicity of QDs both in vivo (Tang et al., 2009) and in vitro has been reported, even if the most severe effects are related to bare CdSe nanoparticles (Tang et al., 2008a, 2008b).

2. Materials and Methods

2.1. QDs samples

Qdot® 525 ITK™ carboxyl and Qdot® 585 ITK™ carboxyl quantum dots from Invitrogen (Carlsbad, CA), here called for brevity QDs 525 and QDs 585, are characterized by a maximum of emission at 525 and 585 nm respectively. These materials are core/shell CdSe/ZnS quantum dots further coated with a polymer layer which increases water solubility while preserving the optical properties of the materials. The polymer coating has $–COO^-$ surface groups available for modifications such as macromolecule attachment. Invitrogen declared the nature of the polymer as confidential. As stated by the supplier, QDs diameters are in the range 10-20 nm.
Qdots are shipped at the concentration of 8 μM in a borate buffered solution (50 mM, pH 9). The dimensions of the studied QDs are about the size of a large macromolecule or protein as declared by Invitrogen.

2.2. Biosimulated fluids

2.2.1. Neutral cellular simulant fluid (NCSF)

The neutral cellular simulant fluid without proteins (NCSF, pH 7.6) is derived from Gamble's solution (Scholze and Conradt, 1987), slightly modified. The chemical composition of the solution is reported in Table 1. The pH was adjusted to 7.6 by bubbling CO_2 in the solution.

2.2.2. Acidic cellular simulant fluid (ACSF)

A 0.02 M potassium hydrogen phthalate (KHP)-buffered ACSF was derived from phagolysosomal simulant fluid (Stefaniak et al., 2005), slightly modified. The chemical composition of ACSF (pH 4.6) is reported in table 2.

In both NCSF and ACSF ultrapure MilliQ (Millipore, Billerica, MA, USA) water was used to prepare the buffer and sodium azide (0.1%) was added in order to prevent the growth of algae or bacteria.

2.3. Ion release in biosimulated fluids

The release of ions was studied under static leaching conditions in the biosimulated fluids. The QDs were suspended in either NCSF or ACSF (QDs final concentration: 4 nM). In order to assess the stability of the polymer capped ZnS/CdSe QDs in conditions which possibly decrease the capping effectiveness in preventing ion release, some suspensions of QDs in NCSF and ACSF were sonicated for 5 minutes with a probe sonicator (33 W, 20 Hz, Bandelin, Berlin, Germany) in an ice-bath and UV irradiated for 30 minutes (500 W mercury/xenon lamp, Oriel instruments, equipped with a IR water filter to avoid overheating of the suspensions). After an incubation of 72 h at 37°C in the dark, the suspensions were filtered on a cellulose acetate filter membrane (cutoff 3 kDa) and the amount of cadmium and zinc in the supernatant was measured by means of ICP-AES technique. All the experiments were carried out at least twice.

2.4. Inductively coupled plasma atomic emission spectrometry

Inductively coupled plasma atomic emission spectrometry ICP-AES analyses of cadmium and zinc were performed with an IRIS II Advantage/1000 Radial Plasma Spectrometer by Thermo-Jarrel Ash Corp. The optical system is sealed with inert gas, with no moving parts, high resolution (ER/S) capable. The Echelle grating & Dispersion prism monochromator range extends between 165 and 800 nm, with an optical resolution of 0.007 nm (at 200 nm). The photo device is a Charge Injection Device Camera frozen to -50 ºC.

2.5. Cell cultures and Quantum Dots incorporation

GT1-7 cells (generously donated by Prof. P.L. Mellon) were cultured either in the presence or in the absence (control conditions) of QDs 525 and QDs 585 (1/500, corresponding to a concentration of 16 nM) in a standard culture medium, DMEM with added 10% fetal bovine serum (FBS, Lonza, Basel, Switzerland). The concentration used in these experiments is on the low side of the doses reported to exert toxic effects on other cellular models (se e.g. Clift et al., 2010). Cells were fixed in 4% Paraformaldehyde (PAF) for 20 min at room temperature after 24, 48 and 72 h in culture and then incubated overnight at 4 °C with a monoclonal anti-β-Tubulin III (anti-β-TubIII) antibody (1:500). The reaction was developed with an anti-mouse IgG Cy3 conjugated antibody, produced in sheep, for cells treated with QDs 525, while for double staining with QDs 585, cells were incubated with a goat biotinylated anti-mouse IgG (Vector Laboratories, Burlingame, CA; 1:200) and detected with the Avidin-FITC complex (Vector Laboratories; 1:400). Images (1024 X 1024 pixels, 16-bit gray scale) were acquired by means of a Fluoview 200 laser scanning confocal microscope (Olympus America Inc., Melville, NY, USA) with 60X and 100X objectives, at excitation

wavelengths of 568 and 488 nm. For each field, both the fluorescent and the differential interference contrast (DIC) images were acquired. Images were acquired in XYZ planes, and subsequent 3D reconstructions were performed in order to check the internalization of QDs. Image analysis was performed using the image processing and analysis program ImageJ (Rasband, 2009). Three independent experiments (each in duplicate) were performed.

A second set of experiments was performed to check if QDs incorporated into the cells following a 24 h or a 48 h incubation were still present intracellularly at 72 h or they were extruded by exocytotic mechanisms. Culture conditions, QDs concentrations, cellular staining and image acquisition were the same as above. Two independent experiments (each in duplicate) were performed.

2.6. Cytotoxicity tests

For survival and proliferation assays GT1–7 cells were seeded on uncoated plastic dishes (Falcon, Becton Dickinson, Franklin Lakes, NJ, USA), at a density of 30.000 cells/cm^2 and maintained in Dulbecco's Modified Eagle's medium (DMEM, Sigma) supplemented with either 10% or 0.5% FBS, 50 μg/ml gentamycin and 2 mM glutamine, at 37 °C, in a humidified atmosphere of 5% CO_2 in air. 10% FBS is the standard culture condition used in order to obtain exponential growth; 0.5% FBS is the concentration that allows survival with reduced proliferation.

Cells were incubated, 24 h after seeding, with either QDs 525 or QDs 585. Cytotoxicity was evaluated by counting cells with a Burker chamber at 24 and 72 h after incubation with QDs and in control conditions (no QDs added to the medium). Each experiment was made in duplicate; three independent experiments were performed for each individual treatment.

2.7. Lysosomal incorporation

To visualize localization of QDs in lysosomal compartments, GT1-7 cells were stained with the targeted fluorescent marker Lysotracker Red DND-99 (Invitrogen). Following 72 h in culture in the presence of green QDs 525, cells were incubated for 5 min in Lysotracker Red and subsequently fixed in 4% PAF. Three independent experiments were performed. Images were analyzed with the Olympus Fluoview 200 confocal microscope as described above.

2.8. Statistical analysis

Where appropriate, data are expressed as mean ± standard error of the mean (SEM). Statistical analysis in citotoxicity experiments was performed by comparing, at each time point, the different treatments with control groups by means of the ANOVA model and related post hoc tests (with

Bonferroni correction). The software employed for the analysis was SPSS version 14.0 for Windows (SPSS Inc., Chicago, USA).

3. Results

3.1. Non-functionalized QDs can be stably incorporated into neuronal cells

In order to assess the capability of the neuronal cells to incorporate coated but non functionalized QDs, GT1-7 cells were incubated with the QDs, marked with beta-tubulin and then analyzed by means of confocal microscopy.

In Fig. 1 (panels A1-3) it can be seen that after 48h of incubation, some cells have incorporated green QDs 525, that appear as spots likely representing aggregates of QDs. Comparable results were obtained for incubation times of 24 and 72 h (not shown).

Similar results were also obtained with the QDs 585. In this case (Fig. 1, panels B1-3) the internalization was more marked and diffuse. Again comparable results were obtained for incubation times of 24, 48 and 72 h.

A further series of experiments was aimed at evaluating whether the QDs incorporated within the GT1-7 cells following a 24 or 48 h incubation were stably retained or subject to exocytotic externalization.

In cells incubated for either 24 or 48 h with QDs 585, the presence of the nanoparticles could be detected after 72 h in culture, thus providing evidence for a stable incorporation.

Fig. 1 (panels C1-3) shows an example of two GT1-7 cells incubated for 24 h with QDs 585: several red spots can be observed inside the cells.

3.2. Localization of QDs into lysosomal compartments

After having shown that GT1-7 cells can incorporate and retain non-functionalized Quantum Dots, we investigated their subcellular localization with specific focus on acidic lysosomal compartments, by means of the fluorescent marker Lysotracker Red DND-99..

Confocal analysis provides evidence for a limited co-localization of the green signal (QDs) and the red one (Lysotracker Red). Fig. 2 shows a representative example of double staining: points at which co-localization can be observed are represented in yellow in Fig. 2B and in white in Fig. 2C-D. Direct evidence is provided by Fig. 2D, showing a section along the white line in A and B.

Colocalization was observed in 74 cells out of 117 (63%); however, the incorporation into lysosomal compartments was localized to a few spots, corresponding to a low fraction of the whole lysosomal compartment.

3.3. Role of different intracellular milieus in the release of metallic ions from CdSe/ZnS QDs

Many solid particles which do not release their constituent ions in water suspension may release them in biological fluids, hence also in vivo. The action is usually caused by pH variations and/or associated to the presence of endogenous chelators which may extract the less coordinated more prominent ions from the solid structure. Since several authors have reported that toxic effects can be linked to the release of metal ions inside the cells (Derfus et al., 2004; Clift et al., 2010), and that pH can be one of the chemical parameters affecting this process, we tested the release of the two most likely candidates, Cd^{2+} and Zn^{2+}, in the presence of artificial media mimicking the extracellular/cytosolic (neutral pH) and the lysosomal (acidic pH) environments.

After 72 h of incubation in NCSF, no Zn^{2+} or Cd^{2+} release from QDs was detected (table 3), indicating that these polymer capped ZnS/CdSe QDs are stable in a neutral environment. Derfus et al., 2004 observed that photolytic and oxidative conditions (e.g. UV irradiation, presence of oxygen) expose the potentially toxic shell material and core metal components. In order to evaluate the effect of perturbing conditions on the polymer and/or the ZnS capping the QDs suspended in NCSF, we performed a cycle of UV irradiation/sonication. After a 72h incubation the release of metal components was tested. No ion release was observed also in these conditions, highlighting the resistance to dissolution of the QDs studied at the neutral pH of NCSF.

When QDs were incubated in the ACSF (pH= 4.6), both Zn^{2+} and Cd^{2+} were released after incubation (Table 3 and Fig.3). The release of Zn^{2+} and Cd^{2+} from QDs was enhanced by the sonication/UV irradiation process. Moreover QDs 585 released a higher amount of both Zn^{2+} and Cd^{2+} than QDs 525. The concentration of Zn^{2+} was higher than the concentration of Cd^{2+} in all experiments. The significant amount of both Zn^{2+} and Cd^{2+} released after incubation in the ACSF suggests that degradation of the polymeric capping and dissolution of both inorganic components are likely to take place when QDs are accumulated in an acidic compartment such as lysosomes.

3.4. GT1-7 survival and proliferation in the presence of QDs

Having shown that QDs are incorporated albeit to a limited extent in lysosomal compartments where the acidic milieu can induce release of toxic metal ions, we evaluated the effects of incubation with Qdots on GT1-7 viability and proliferative rate. This cell line, while expressing all the basic properties of differentiated cells and of electrically excitable neurons, can also be induced to proliferate in the presence of serum.

To this purpose, cells were incubated for 24, 48 and 72 h with QDs 525 and QDs 585, in the presence of 10% FBS, and their number evaluated at the end of the incubation periods (Fig 4A). For

24 and 48 h incubation, no significant differences can be observed as compared to control cultures maintained in the presence of serum alone (24 h: CTRL 55839 ± 2345 cells/cm^2, QDs525 50579 ± 660 cells/cm^2, QDs585 50664 ± 3313 cells/cm^2; 48 h: CTRL 60771 ± 3130 cells/cm^2, QDs525 58920 ± 3517 cells/cm^2, QDs585 57202 ± 1177 cells/cm^2). At 72 h - when the proliferative effect of serum can be evidenced - a significant reduction in cell number could be observed with both QDs (CTRL 97162 ± 5061 cells/cm^2, QDs525 66977 ± 1822 cells/cm^2, QDs585 64123 ± 4190 cells/cm^2). These data can be interpreted as evidence for a lack of gross cytotoxic effects in the presence of a specific reduction of the proliferative rate of these cells.

A further control was made by repeating the protocol in the presence of 0.5% serum, to check the effects on more differentiated, non proliferating cells. In Fig. 4B only for QDs 525, at 48 and 72 h, a slight but significant reduction in cell number was evidenced, pointing to limited effects on cell survival (24 h: CTRL 41196 ± 4427 cells/cm^2, QDs525 32149 ± 3168 cells/cm^2, QDs585 67801 ± 3903 cells/cm^2; 48 h: CTRL 47406 ± 1584 cells/cm^2, QDs525 34947 ± 888 cells/cm^2, QDs585 42422 ± 3233 cells/cm^2; 72 h: CTRL 42869 ± 3325 cells/cm^2, QDs525 28942 ± 2423 cells/cm^2, QDs585 33893 ± 1629 cells/cm^2).

Finally, after incubation up to 72 h with either QDs 525 or QDs 585 no gross morphological changes could be observed. Fig. 4C shows images representative of three experiments.

4. Discussion

The data obtained in this study provide the first detailed analysis of the incorporation of QDs in neuronal cells, their subcellular localization and toxicity. Neurotoxicity of QDs is a poorly studied issue todate, despite the fact that nanoparticles including QDs can be incorporated through different entry points (mainly the skin and the respiratory tract) and subsequently pass the blood-brain barrier (Simkó and Mattsson, 2010). While the translocation rate is likely to be relatively low, no data are available at present for chronic exposures (Simkó and Mattsson, 2010). It is noteworthy that the only available *in vivo* data point to an impairment of synaptic transmission in rat hippocampal neurons, whose activity and plasticity are related to learning and memory (Tang, et al., 2009).

The cellular tests evidenced the stable internalization of both QDs 525 and QDs 585 into cytosolic and lysosomal compartments. In preliminary experiments, we tested incorporation with different concentrations of QDs, without observing relevant differences (data not shown). The dose used in the experiments reported in this paper was chosen as it corresponds the low side of doses used for *in vivo* and *in vitro* cytotoxicity tests (see e.g. Hauck et al., 2010; Kuo et al., 2011).

We did not investigate in detail the mechanism of incorporation: however, for nanoparticles such as QDs, endocytosis is the best described pathway (Hild et al., 2008). Interestingly, a recent paper

(Aaron et al., 2011) reports that endocytosis and lysosomal sorting increase with particle size. While the extent of incorporation is rather limited, it must be kept in mind that neurons differ from other widely used cellular models such as macrophages (Clift et al., 2010) for a much lower endocytotic activity. Incorporation in other subcellular compartments was not investigated, since the aim of this work was to assess the role of acidic compartments in the potential release of ions by internalized QDs.

In the extracellular and cytosolic environments ion release following the degradation of the polymeric capping may be negligible due to the high stability of the polymeric and/or ZnS capping at neutral pH, as evidenced by the experiments of ion release in NCSF; on the other hand, similarly to what observed in the ACSF, we can expect that metal ions would be released following dissolution of the QDs internalized in the lysosomal vesicles that, in neurons as in other cell types, are characterized by an acidic environment (Overly et al., 1995). The limited lysosomal incorporation of the QDs 525 (Fig.2) can explain the lack of gross cytotoxic effect observed on these neuronal cells. Very limited impairment of cell survival could be observed, and only for QDs 525 at 72 h. Emission wavelengths of QDs increase with nanoparticle diameter, and several reports point to size-dependent toxic effects, smaller particles being more toxic (see e.g. Ariano et al., 2011). On the other hand, both QDs induced a marked reduction of cell proliferation, thus pointing to a specific perturbation of the complex set of signals that control the progression into the cell cycle. Our data refer to times up to three days in culture; a different and more severe picture could emerge for longer exposures.

Our results, therefore, while excluding dramatic neurotoxic effects of CdSe/ZnS QDs, point to the need of more extensive investigation of the mechanisms of interaction of these nanoparticles with neuronal cells and of the ensuing perturbations of cellular functions.

Acknowledgments

We gratefully acknowledge the financial support of the Fondazione CRT, Torino, Project “Potential toxicity of nanoparticles in the nervous system: an integrated approach to the evalution of relevant parameters”. We thank Dr. Federico Alessandro Ruffinatti for help in data analysis.

References

Aaron, J.S., Greene, A.C., Kotula, P.G., Bachand, G.D., Timlin, J.A., 2011. Advanced optical imaging reveals the dependence of particle geometry on interactions between CdSe quantum dots and immune cells. Small. 7, 334-341.

Ariano, P., Zamburlin, P., Gilardino, A., Mortera, R., Onida, B., Tomatis, M., Ghiazza, M., Fubini, B., Lovisolo, D., 2011. Interaction of Spherical Silica Nanoparticles with Neuronal Cells: Size-Dependent Toxicity and Perturbation of Calcium Homeostasis. Small, 6, 766–774.

Akerman, M.E., Chan, W.C., Laakkonen, P., Bhatia, S.N., Ruoslahti, E., 2002. Nanocrystal targeting in vivo. Proc. Natl. Acad. Sci. U.S.A. 99, 12617-12621.

Ballou, B., Lagerholm, B.C., Lauren, L., Ernst, A., Bruchez, M.P. Waggoner, A.S., 2004. Noninvasive imaging of quantum dots in mice. Bioconjugate Chem. 5, 79-86.

Bruchez, M., Moronne, M. Gin, P., Weiss S., Alivisatos A.P., 1998. Semiconductor nanocrystals as fluorescent biological labels. Science 281, 2013-2016.

Chan, W.C., Nie, S., 1998. Quantum dot bioconjugates for ultrasensitive nonisotopic detection. Science 281, 2016-2018.

Chan, W.C., Maxwell, D.J., Gao, X., Bailey, R.E., Han, M., Nie, S., 2002. Luminescent quantum dots for multiplexed biological detection and imaging. Curr. Opin. Biotechnol. 13, 40-46.

Clift, M.J.D., Varet, J., Hankin, S.M., Brownlee, B., Davidson, A.M., Brandenberger, C., Rothen-Rutishauser, B., Brown, D.M., Stone, V. 2010. Quantum dot cytotoxicity in vitro: An investigation into the cytotoxic effects of a series of different surface chemistries and their core/shell materials. Nanotoxicology, Early Online, 1–11.

Derfus, A.M., Chan, W.C., Bhatia, S., 2004. Probing the cytotoxicity of semiconductor quantum dots. Nano Lett. 4, 11-18.

Dubertret, B., Skourides, P., Norris, D.J., Noireaux, V., Brivanlou, A.H., Libchaber, A., 2002. In vivo imaging of quantum dots encapsulated in phospholipid micelles. Science 298, 1759-1762.

Hauck, T.S., Anderson, R.E., Fischer, H.C., Newbigging, S., Chan, W.C., 2010. In vivo quantum-dot toxicity assessment. Small 6, 138-144.

Hild, W.A., Breunig, M., Goepferich, A., 2008. Quantum dots - nano-sized probes for the exploration of cellular and intracellular targeting. Eur J Pharm Biopharm. 68, 153-168.

Hoshino, A., Manabe, N., Fujioka, K., Suzuki, K., Yasuhara, M., Yamamoto, K., 2007. Use of fluorescent quantum dot bioconjugates for cellular imaging of immune cells, cell organelle labeling,

and nanomedicine: surface modification regulates biological function, including cytotoxicity. J. Artif. Organs 10, 149–157.

Ipe B.I., Lehnig M., Niemeyer C.M., 2005. On the generation of free radical species from quantum dots. Small 1, 706-709.

Kirchner, C., Liedl, T., Kureda, S., Pellegrino, T., Munoz Javier, A., Gaub, H.E., Stolzle, S., Fertif, N., Parak, W.J., 2005. Cytotoxicity of colloidal CdSe and CdSe/ZnS nanoparticles. Nano Lett. 5, 331-338.

Kuo, T.R., Lee, C.F., Lin, S.J., Dong, C.Y., Chen, C.C., Tan, H.Y., 2011. Studies of intracorneal distribution and cytotoxicity of quantum dots: risk assessment of eye exposure. Chem Res Toxicol. 24, 253-261.

Larson, D.R., Zipfel, W.R, Williams, R.M., Clark, S.W., Bruchez, M.P., Wise, F.W., Webb, W.W., 2003. Water-soluble quantum dots for multiphoton fluorescence imaging in vivo. Science 300, 1434-1436.

Lewinski, N., Colvin, V., Drezek, R., 2008. Cytotoxicity of Nanoparticles. Small, 4, 26 – 49.

Mahendra, S., Zhu, H., Colvin, V.L., Alvarez, P.J., 2008. Quantum dot weathering results in microbial toxicity. Environ. Sci. Technol. 42, 9424–9430.

Muller, K.H., Kulkarni, J., Motskin, M., Goode, A., Winship, P., Skepper, J.N., Ryan, M.P., Porter, A.E., 2010. pH-dependent toxicity of high aspect ratio ZnO nanowires in macrophages due to intracellular dissolution. ACS Nano 4, 6767–6779.

Overly, C.C., Lee, K.D., Berthiaume, E., Hollenbeck, P.J., 1995. Quantitative Measurement of Intraorganelle pH in the Endosomal-Lysosomal Pathway inNeurons by Using Ratiometric Imaging with Pyranine. Proc. Natl. Acad. Sci. U.S.A. 92, 3156-3160.

Praetner, M., Rehberg, M., Bihari, P., Lerchenberger, M., Uhl, B., Holzer, M., Eichhorn, M.E., Fürst, R., Perisic, T., Reichel, C.A., Welsch, U., Krombach, F., 2010. The contribution of the capillary endothelium to blood clearance and tissue deposition of anionic quantum dots in vivo. Biomaterials 31, 6692-6700.

Rasband, W. S., 1997-2009. ImageJ, U. S. National Institutes of Health,Bethesda, Maryland, USA, http://rsb.info.nih.gov/ij/.

Ryman-Rasmussen, J.P., Riviere, J.E., Monteiro-Riviere, N.A., 2007. Surface coatings determine cytotoxicity and irritation potential of quantum dot nanoparticles in epidermal keratinocytes. J. Invest. Dermatol. 127, 143–153.

Rzigalinski, B.A., Strobl, J.S., 2009. Cadmium-containing nanoparticles: perspectives on pharmacology and toxicology of quantum dots. Toxicol. Applied Pharmacol. 238, 280-288.

Simkó M., Mattsson, M.O., 2010. Risks from accidental exposures to engineered nanoparticles and neurological health effects: a critical review. Risks from accidental exposures to engineered nanoparticles and neurological health effects: a critical review. Part. Fibre Toxicol. 21, 7-42.

Scholze H., Conradt, R., 1987. An *In Vitro* Study Of The Chemical Durability Of Siliceous Fibres, Ann Occup Hyg., 31(4B), 683-692.

Stefaniak A.B., Guilmette, R.A., Day, G.A., Hoover, M.D., Breysse, P.N., Scripsick, R.C., 2005. Characterization of phagolysosomal simulant fluid for study of beryllium aerosol particle dissolution. Toxicol. in vitro 19, 123-134.

Tang, M., Wang, M., Xing, T., Zeng, J., Wang, H., Ruan, D.Y. 2008a. Mechanisms of unmodified CdSe quantum dot-induced elevation of cytoplasmic calcium levels in primary cultures of rat hippocampal neurons. Biomaterials 29, 4383-4391.

Tang, M., Xing, T., Zeng, J., Wang, H., Li, C., Yin, S., Yan, D., Deng, H., Liu, J., Wang, M., Chen, J., Ruan, D.Y., 2008b. Unmodified CdSe quantum dots induce elevation of cytoplasmic calcium levels and impairment of functional properties of sodium channels in rat primary cultured hippocampal neurons. Environ. Health Perspect. 116, 915-922.

Tang, M., Li, Z., Chen, L., Xing, T., Hu, Y., Yang, B., Ruan, D.Y., Sun, F., Wang, M., 2009. The effect of quantum dots on synaptic transmission and plasticity in the hippocampal dentate gyrus area of anesthetized rats. Biomaterials. 30, 4948-4955.

Yang, X.Q., Chen, C., Peng, C.W., Hou, J.X., Liu, S.P., Qi, C.B., Gong, Y.P., Zhu, X.B., Pang, D.W., Li, Y., 2011. Quantum dot-based quantitative immunofluorescence detection and spectrum analysis of epidermal growth factor receptor in breast cancer tissue arrays. Int. J. Nanomed. 6, 2265–2273.

Zhang, T., Stilwell, J.L., Gerion, D., Ding, L., Elboudwarej, O., Cooke, P.A., Gray, J.W., Alivisatos, A.P., Chen, F.F., 2006. Cellular effect of high doses of silica-coated quantum dot profiled with high throughput gene expression analysis and high content cellomics measurements. Nano Lett. 6, 800–808.

Figure legends

Fig. 1

Incorporation of QDs in GT1-7 neuronal cells

A1. 3D reconstruction of a XYZ scan of a field of GT1-7 cells incubated for 48 h with 16 nM QDs 525 fixed in 4% PAF and subsequently stained with an anti-β-tubulin antibody (red). Green spots present in some cells correspond to aggregates of QDs 525.

B1. 3D reconstruction of a XYZ scan of a field of GT1-7 cells incubated for 72h with 16 nM QDs 585 , fixed in 4% PAF and subsequently stained with an anti β-tubulin antibody (green).

C1. 3D image reconstructed from XYZ scan of cells treated for 24 h with 16 nM Qdots 585 nm, fixed in PAF 4% after 72 h and subsequently stained with an anti-β-tubulin antibody (green) Red spots correspond to QDs 585 nm.

A2, B2, C2. DIC (inteferential contrast) images of the same field as in A1, B1, C1 respectively.

A3, B3, C3. Images obtained by a virtual section along the white lines in A1, B1, C1 of the same fields scanned on XYZ planes respectively.

Fig. 2

QDs localization in the lysosomal compartment

A. 3D reconstruction of a XYZ scan acquired at the confocal microscope of GT1-7 cells cultured for 72 h in the presence of 16 nM QDs 525, subsequently stained with Lysotracker Red (50 nM) for 5 min and fixed in 4%. PAF. Green spots correspond to Quantum Dots, lysosomal staining is in red.

B. Area outlined by the rectangle in A viewed at higher magnification. Single XY scan. From left: Lysotracker Red staining, QDs 525 staining, colocalization of the two signals.

C. DIC image of the same field as in A. White spots indicate colocalization of red and green signal in A.

Fig. 3

Release of metallic ions from QDs in biosimulated fluids

Zn^{2+} and Cd^{2+} release (μmol/l) after 72 h of incubation at 37°C in ACSF from (A) QDs 525 and QDs 585 and (B) from QDs 525 and QDs 585 sonicated and UV irradiated before incubation. Values are given as means ± SEM.

Fig. 4

Effects of QDs incubation on survival, proliferation and morphology of GT1-7 cells

A. Number of cells in culture after 24, 48, e 72 h, in control conditions (CTRL - DMEM+10% FBS) or in the continuous presence of 16 nM QDs 525 and QDs 585.

B. Number of cells in culture with the same protocols as in A but in the presence of DMEM+0.5% FBS. Here and in A, data represent means ± SEM. from three independent experiments.

** $p<0.01$; * $p<0.05$ vs CTRL conditions at 72 h. $^{++}$ $p<0.01$ vs CTRL condition at 48 h.

C. Phase contrast images of GT1-7 cells cultured for 72 h in control conditions (CTRL - DMEM+10% FBS; left panel) in the continuous presence of 16 nM QDs 525 (middle panel) and QDs 585 (right panel).

Table(s)

Table 1

Composition of the Neutral Cellular Simulant Fluid (NCSF)

Component concentration	(mg/l)
Na_2HPO_4	142.0
NaCl	6650.0
Na_2SO_4	71.0
$CaCl_2 \cdot 2H_2O$	29.0
Glycine	450.0
K hydrogen phthalate	4084.6

Table(s)

Table 2

Composition of the Acidic Cellular Simulant Fluid (ACSF)

Component concentration	(mg/l)
$MgCl_2 \cdot 6H_2O$	212
NaCl	6415
$CaCl_2 \cdot 4H_2O$	318
$Na_2SO_4 \cdot 10H_2O$	179
Na_2HPO_4	148
$NaHCO_3$	2703
(Na_2 tartrate)$\cdot 2H_2O$	180
(Na_3 citrate)$\cdot 2H_2O$	144
Na lactate	175
Glycine	118
Na pyruvate	172

Table 3

Ion release (μmol/l) from QDs 525 and QDs 585 after 72 hours of incubation in neutral cellular simulant fluid (NCSF) and acidic cellular simulant fluid (ACSF). Values are expressed as means ± SEM.

Ion release in NCSF		
sample	**Zn^{2+} (μmol/l)[a]**	**Cd^{2+} (μmol/l) [a]**
QDs 525	nd	nd
QDs 585	nd	nd
QDs 525 sonicated+UV irradiated	nd	nd
QDs 585 sonicated+UV irradiated	nd	nd

Ion release in ACSF		
sample	**Zn^{2+} (μmol/l)**	**Cd^{2+} (μmol/l)**
QDs 525	1.14679 ± 0.07645	0.16964 ± 0.00893
QDs 585	1.86544 ± 0.09174	0.33482 ±0.04911
QDs 525 sonicated+UV irradiated	3.21865 ± 0.00765	0.33929 ±0.04464
QDs 585 sonicated+UV irradiated	2.72171 ± 0.03058	1.59821 ± 0.09821

[a] nd: not detected.

Figure(s)

Click here to download high resolution image

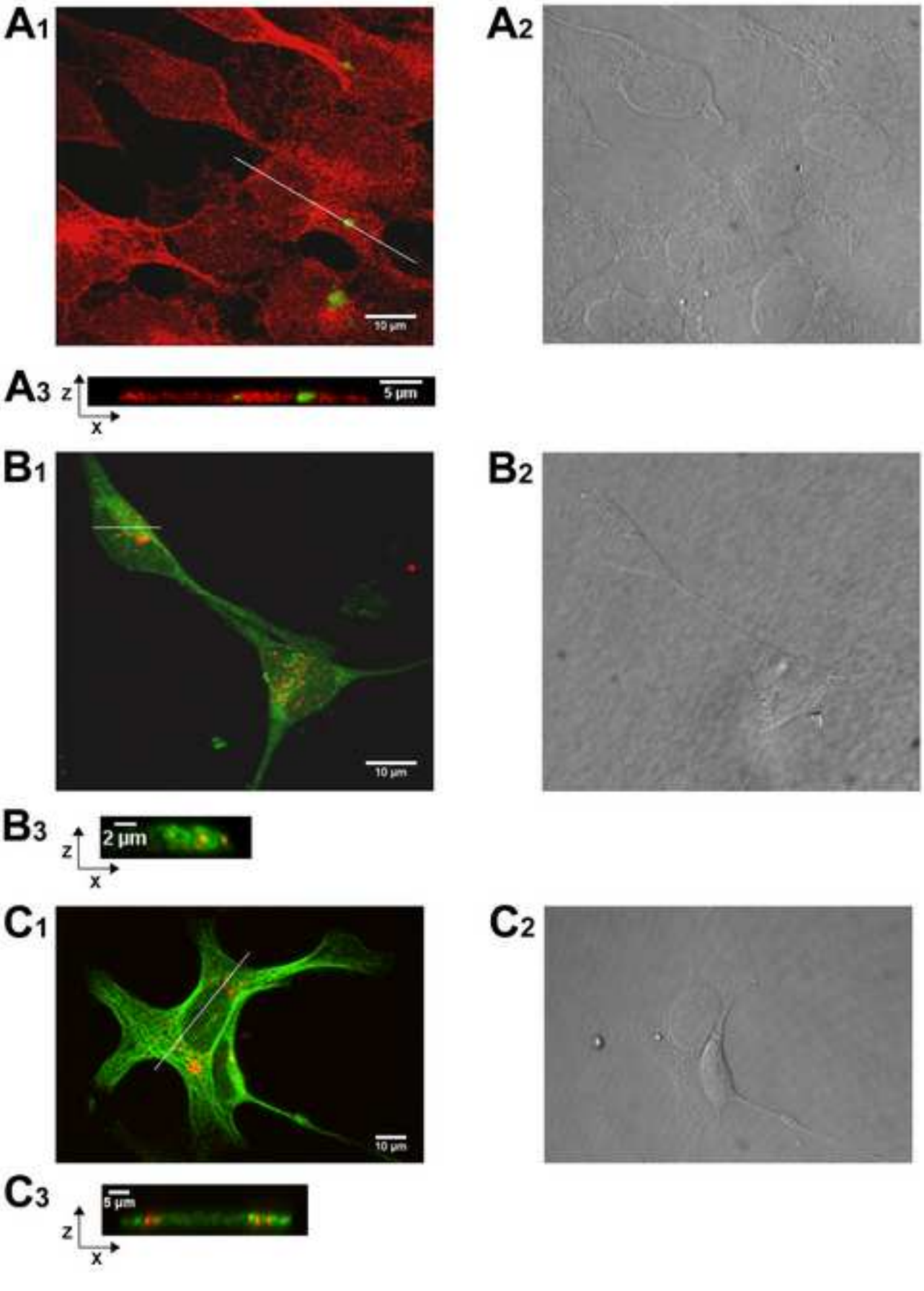

Figure(s)

Click here to download high resolution image

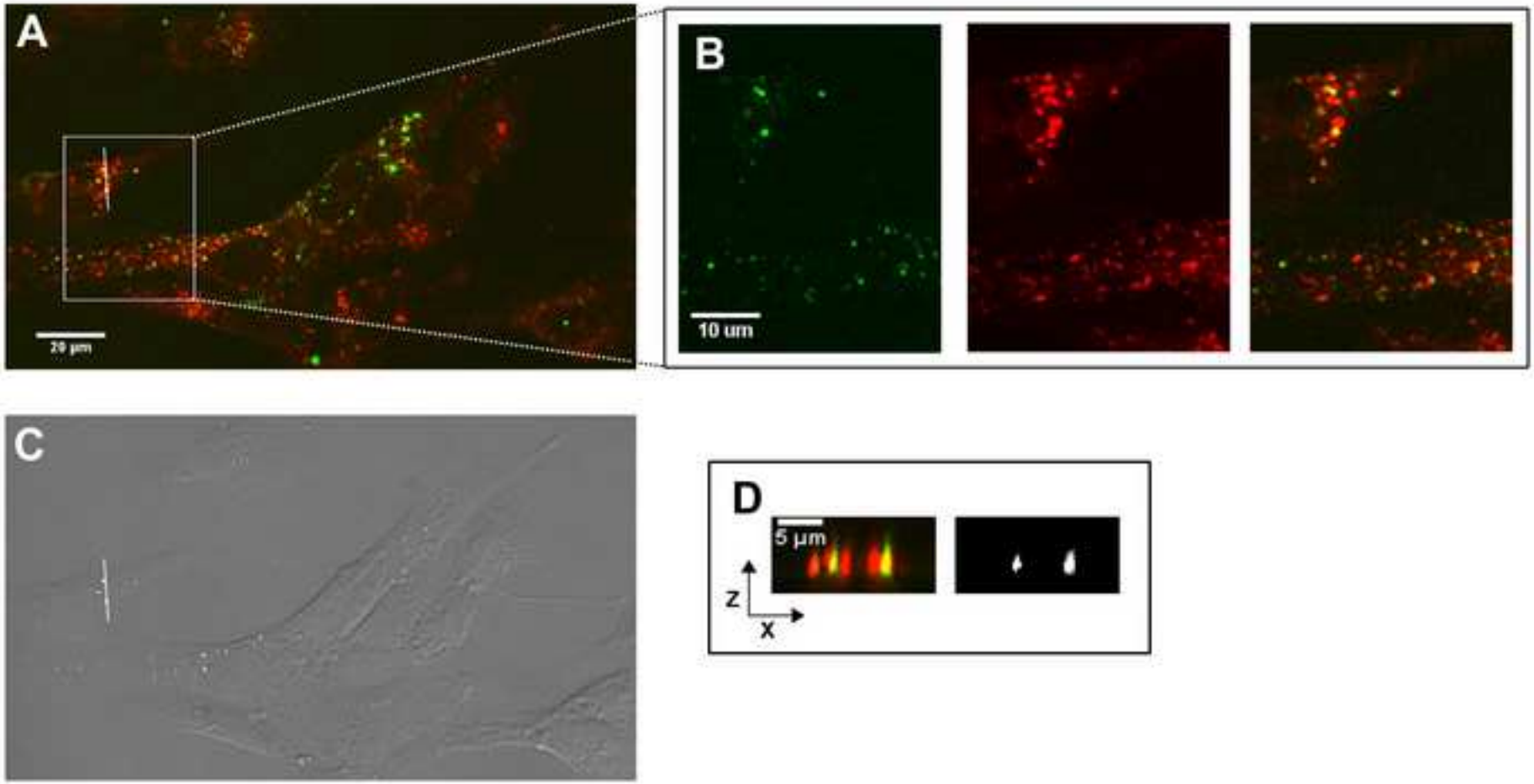

Figure(s)

Click here to download high resolution image

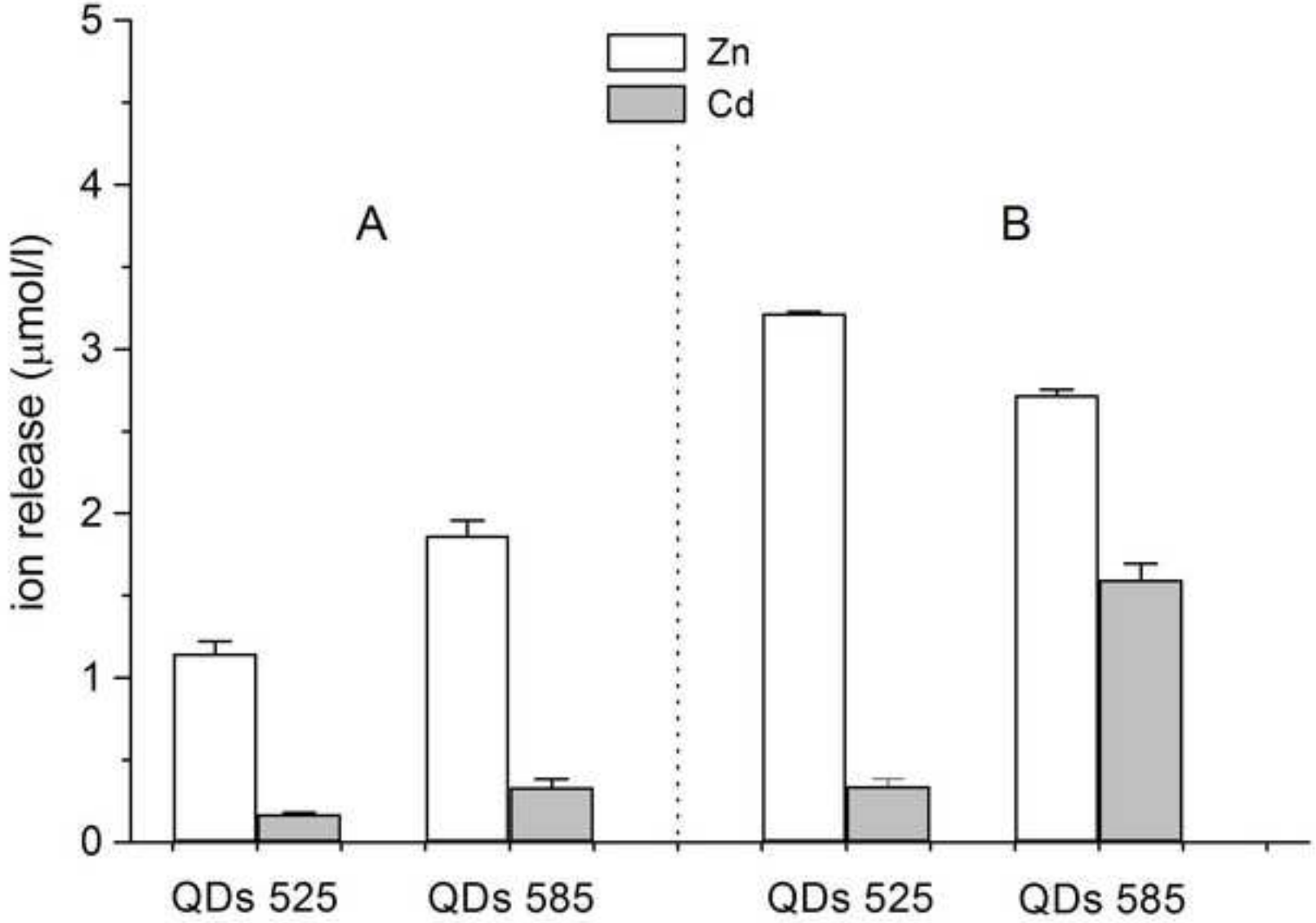

Figure(s)

Click here to download high resolution image